Section A-Research paper
ISSN 2063-5346

Investigation of Structural, Dielectric and Multiferroicproperties of Gd substituted $BiFeO_3$ Nanostructures

Monika[1], S. K. Chaudhary[1], Sunil Rohilla[2], Praveen Kumar[3] and Varun Sangwan[4]

[1]Department of Physics, Baba Mastnath University, Rohtak (India) -124021

[2]Department of Physics, C. R. S. University, Jind (India) -126102

[3]Department of Physics, Govt. College for Women, Tosham(India) -127040

[4]Department of Electronics and Communication, Delhi Technological University, New Delhi (India)-110042

Corresponding Author – Monika (monikalohchab3333@gmail.com)

Article History: Received: 20.08.2023 Revised: 01.09.2023 Accepted: 10.09.2023

Abstract:

In this paper polycrystalline sample of Gd/$BiFeO_3$ (at Gd concentration X= 0.20) were synthesized in solid-state reaction process. The present study inquiries effect of temperature, frequency and addition of Gd/$BiFeO_3$ on structural, dielectric and multiferroic properties. Crystalline nature of organized samples was definite by the X-ray diffraction procedure. The domain size calculated by scherrer's formula is 19.64 nm. Dielectric studies are carried out at frequencies ranging from 10 Hz to 1 MHz. Dielectric analysis of the samples reveals that the samples with the lowest dielectric constant at lower frequencies. High concentrations of Gd cause an improvement in the values of dielectric continuous and dielectric loss. Asymmetric semi-circular arcs are visible on modulus a spectroscopy plot, which supports the existence of the dielectric relaxation phenomenon.The PE and MH studies are carried out at room temperature (300 K) and the values of saturation polarization (P_s) and magnetization (M_s) was found 2.256 μC/cm^2 and2.614 emu/gm, respectively.

Keyword: Gd doping, Solid State route, Impedance, Saturation Polarization, Saturation Magnatization.

1. Introduction: -

Multiferroics are a remarkable class of resources that can have two or extra ferromagnetic, ferroelectric, and ferroelastic properties integrated in a single phase. Magnetoelectric compounds are multiferroics that possess ferroelectric and ferromagnetic characteristics [1]. The submission of an electric field can produce a magnetic field in a magnetoelectric compound, and the introduction of a magnetic field can cause polarization. The introduction of coupling between ferroelectric and ferromagnetic properties provides enhanced physical qualities as well as a broad range of industrial applications such as statistics storage, spintronics, transducers, instruments, and so on[2-3]. Bismuth ferrite is single of the most prominent multiferroic materials, with an anti-ferromagnetic Neel temperature of 643K and aextraordinary ferroelectric transition temperature of 1103K, and it has G type AFM ordering[4]. The unfilled d orbits of Fe3+ ions cause antiferromagnetic behavior in BiFeO3, whereas the lone pair of electrons in 6s Bi3+ ions cause ferroelectric performance [5]. Bismuth ferrite crystallizes in a rhombohedral deformed perovskiteconstruction with R3c space group and hexagonal symmetry

[6].Bismuth ferrite is a promising contender for numerous applications; nevertheless, due to the presence of inferior phases such as $Bi_{24}Fe_2O_{39}$ and $Bi_2Fe_4O_9$[7-8,] it takes considerable effort to synthesize single phase substrate free nanoparticles of bismuth ferrite. The majority of the studies presented in the literature demonstrate the occurrence of impurity phases in various samples [9]. Second, the leakage current demonstrated by these Bi multiferroics is substantial, but the fundamental issue is low magnetization in bulk due to the spiral modulated spin period of 62nm[10], which prevents the P-E loop from being saturate. These constraints limit the use of bismuth multiferroic as a multifunctional device application. Several scientists experimented with various methods to solve these problems.To improve themultiferroic properties of bismuth ferrites it is doped on the A site (Bi site) thru rare earth elements with valency 3+ such as Gd, La, Ce, etc. and alkaline earth elements with valency 2+ such as Mg, Sn, Ti, etc. [4, 11-12]. Various transition metal elements, such as Mn, Se, Cr, and Zn, were doped at B sites (Fe sites) by various scientists to boost magnetization value[13-15].In this work we focused on the Gd doping in $BiFeO_3$ nanostructures for enhancement in structural, dielectric and multiferroic properties.

2.Experimental:

The multiferroics having the composition $Bi_{0.80}Gd_{0.20}FeO_3$, were synthesised using a solid state reaction technique. For the manufacture of the aforementioned samples, high quality Bismuth oxide (Bi_2O_3), iron oxide (Fe_2O_3), and Gadolinium oxide (Gd_2O_3) chemicals were utilised. All of the ingredients listed above were carefully weighed in stochiometric amounts and pulverised into very fine powder using an agate mortar until a homogenous mixture was created. The prepared homogenous combination of samples was calcined high temprature for 2 hours before being reground into a fine mixture. The resultant sample combination was then palletized and heat treated for 4 hours.

3.Results and Discussion:

3.1 Structural and Morphological Analysis:

X-ray diffraction (XRD) was used to do structural study on as obtained Nd doped Bismith mutiferroic synthesised by solid state reaction technique. Figure 1illustrations the XRD pattern of prepared multiferroics, with sharp, highly intensed, well defined, and strong diffraction peaks for all prepared samples, confirming that they are all extremely crystalline in nature. The presence of the compound is confirmed by the peak obtained from the XRD pattern [16-17].

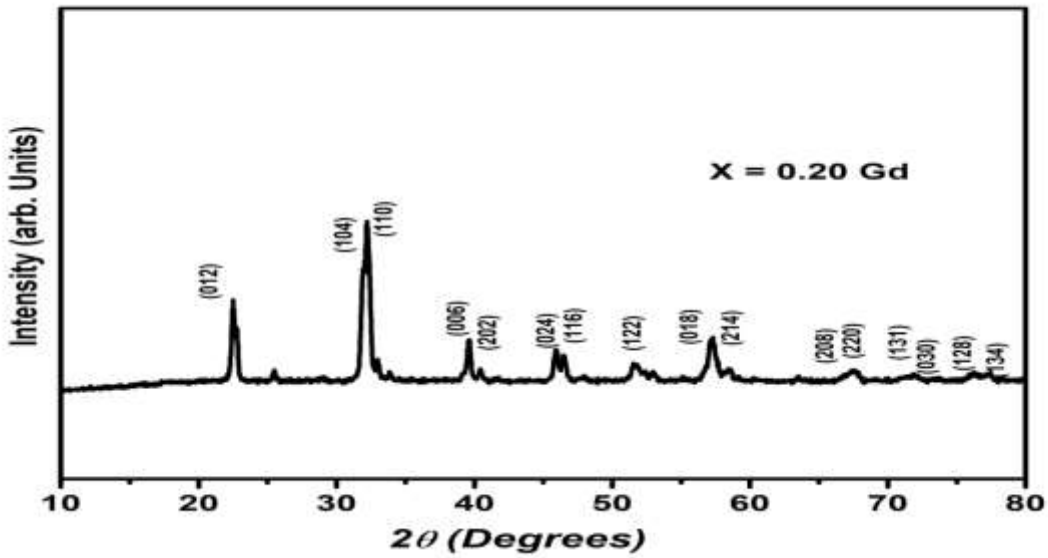

Figure 1: XRD patterns of Gd (X = 0.20) doped $BiFeO_3$ nanostructure.

FESEM is a sophisticated instrument for determining sample grain size. Figures 2 demonstrate the effect of Gd on the morphology of $Bi_{0.80}Gd_{0.20}FeO_3$ obtained by FESEM. Figures 2 indicate that the inclusion of Gd systametically filled the pores on the surface of the nanoparticles, resulting in a $BiFeO_3$-$GdFeO_3$ nanocomposite. The FESEM images reveal that the prepared samples have irregular shapes and sizes. For prepared samples, the average grain size is a few micrometres, and grain size decreases as Gd concentration increases. This type of grain size reduction is acceptable due to phase transformation with increasing Nd replacement and has also been observed in the literature [17-18].

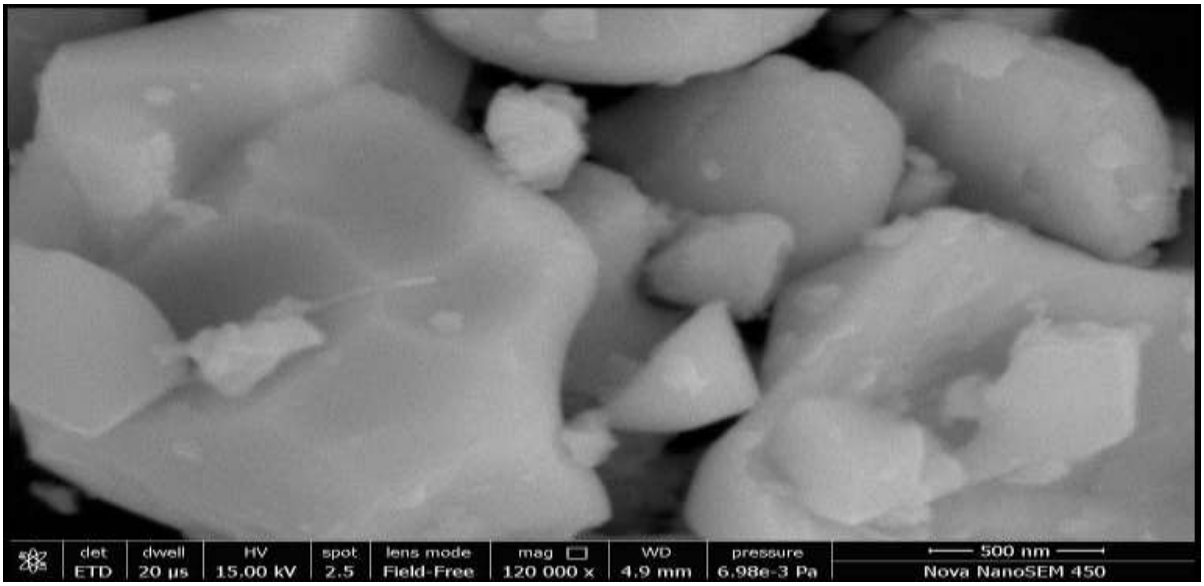

Figure 2: FeSEM micrograph of $Bi_{0.80}Gd_{0.20}FeO_3$ nanostructure.

3.2Dielectric Analysis:

3.3.1 Dielectric constant:

Figure 3 depicts the fluctuation of the real component of the dielectric constant (') vs frequency at different temperatures for bismuth multiferroicswith Gd doping concentrations (X = 0.20). The difference of the real component of the dielectric constant with frequency at various temperatures displays a similar pattern. The worth of the dielectric incessant decreases rapidly with increasing frequency at first, then approaches a virtually constant value for the processed samples about logω = 4 (Hz) [19-20].At low frequencies, defect-related dipoles can follow alternating current, resulting in a high dielectric constant, indicating a significant dielectric dispersion area.

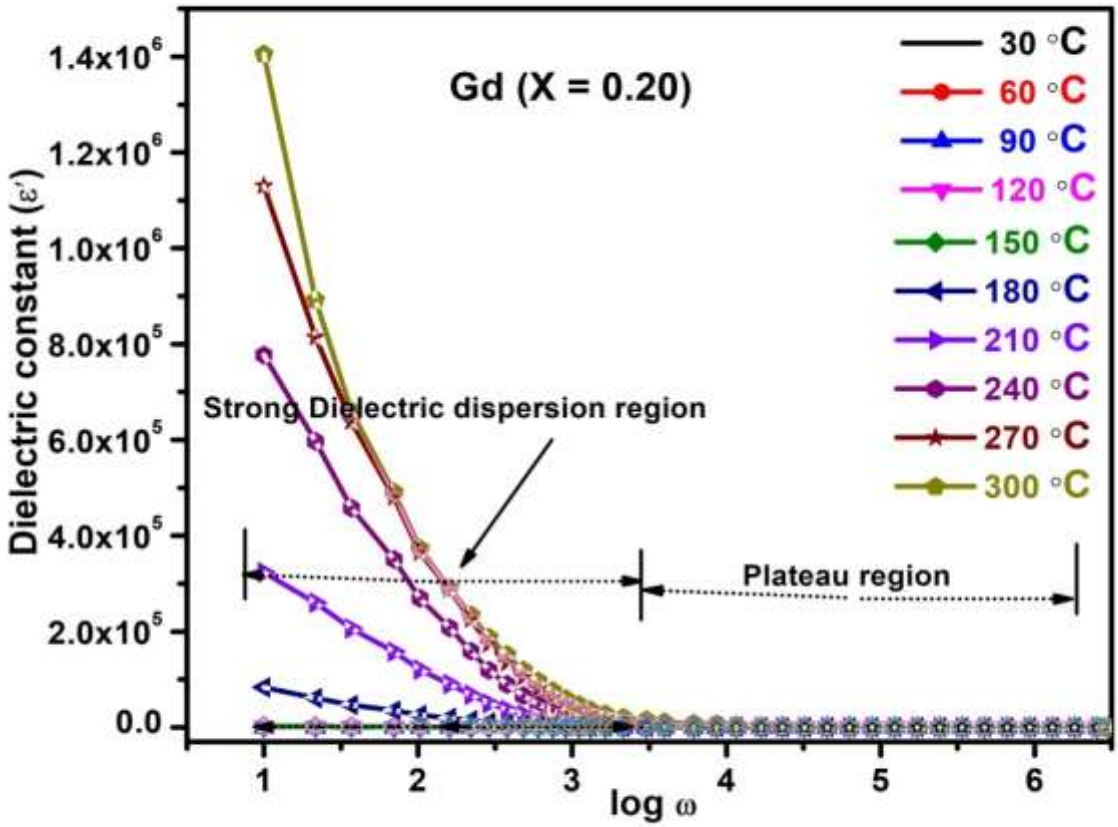

Figure 3: Variation of dielectric constant with frequencies at various temperature values.

As frequency increases, dipoles begin to lag behind the applied field, and the dielectric constant drops, i.e., plateau area, finally reaching a specific frequency after which dielectric constants display practically constant value. The plateau region acquired for the composition sample (Gd = 0.20), appears more frequently than the plateau regions produced for the other three synthesized composition samples. This type of conduct is consistent with Koop's phenomenological theory and demonstrates consistency with

the interfacial polarization of Maxwell Wagner type. According to the Maxwell Wagner model, at lower frequencies, grain boundaries and charge defects contribute more because dielectric constants exhibit a diminishing trend, but conducting grains are more dominating at higher frequencies [18, 20-22].

3.3.2Conductivity:

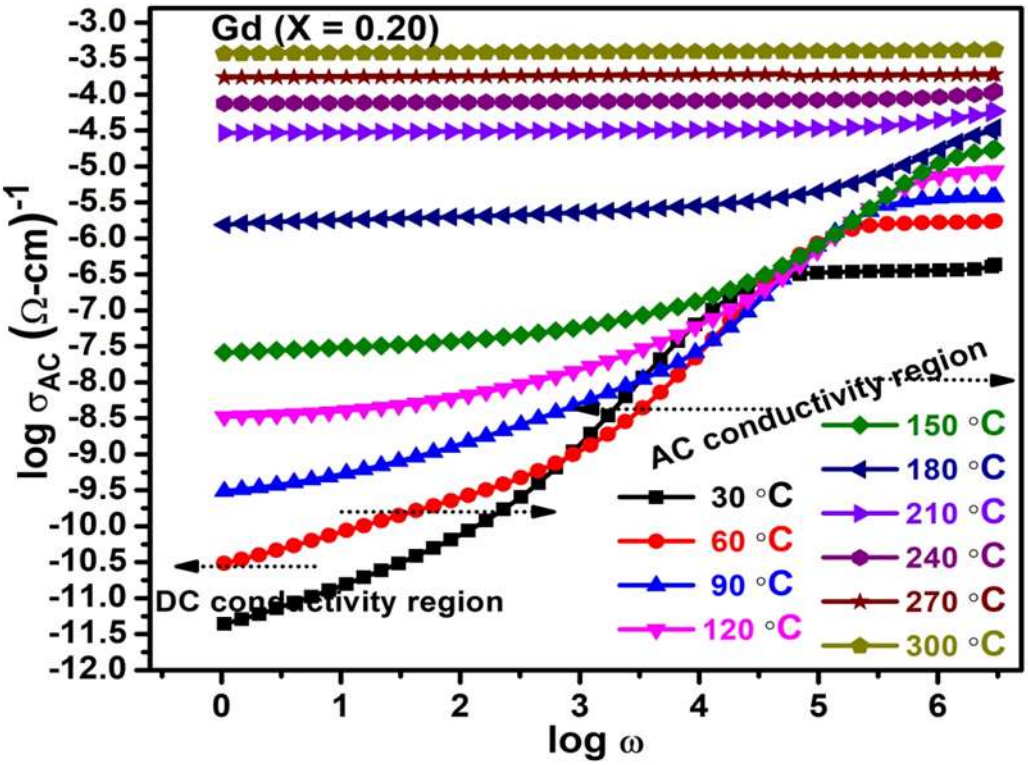

Figure 4: Variation of Ac conductivity with frequency at various temperature values.

To further understand the conduction process in multiferroic conductivity experiments for varied concentrations of Nd in bismuth multiferroic were also performed. Figure 4 depicts the exponential variation of conductivity for several samples from 10 Hz to 1 MHz.Figure 4 clearly indicates that conductivity for all produced samples exhibits nearly independent behavior at low frequencies, followed by a dramatic increase. The following relationship can be used to describe the conductivity relationship.

$\sigma_{AC}(\omega) = \omega \varepsilon_o \varepsilon' \tan\delta$ ..... (1)

Where, ε_o is the free space permittivity, and tanδ is the dielectric loss. A similar pattern of behavior is observed for La doped bismuth multiferroic [21]. The obtained results for AC conductivity with temperature demonstrate that at low temperatures, it is essentially constant and then increases for all samples. Thermally activated charge carriers and charge defects contribute more to increased conductivity at high temperatures[22]. At low frequencies, as demonstrated in figure 4, conductivity is frequency independent and is attributed to DC conductivity.

Electric field – Polarization (P-E) studies:

The electric field dependent polarisation (P-E loops) studies of Gd doped $BiFeO_3$ (x = 0.20) at ambient temperature as a function of frequency are depicted in Figure 5. The outcomes show that as the Gd concentration in $BiFeO_3$ increased relative to undoped BFO, the profile of P-E loops (typical and saturated P-E loops) improved dramatically due to a drop in leakage current. Pure BFO, on the other hand, contains roundish unsaturated P-E loops that can be caused by significant leakage currents and coercive fields [17, 19]. For the Gd doped BFO (x = 0.20) sample, the maximal saturation polarization (P_s) and remanent polarization ($2P_r$) values are 2.256 and 1.24μC/cm^2, respectively. The plots also show the comparative changes in saturation polarization values, revealing the somewhat better ferroelectric characteristics due to Gd doping. Charge defects, secondary phases, and non-stoichiometry all contributed to this type of phenomenon. Furthermore, when Gd doping increases, so does the density of the leakage current.Another factor is the suppression of oxygen vacancies generated by Gd doping, as O_2vacancies are important for ferroelectric domain pinning [23]. Furthermore, Gd doping on the Bi-site results in FeO_6 octahedron deformation (change in Fe-O link lengths), which may improve the ferroelectricity of Gd doped BFO (x = 0.20) samples.

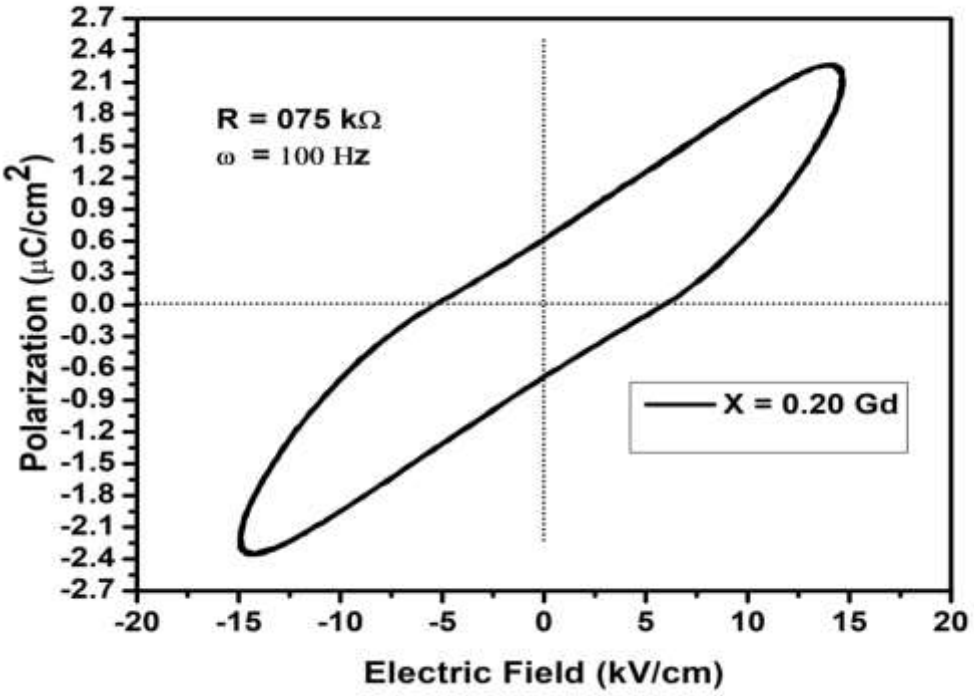

Figure 5: P-E Hysteresis loop of Gd(X = 0.20) doped $BiFeO_3$

VSM Analysis:

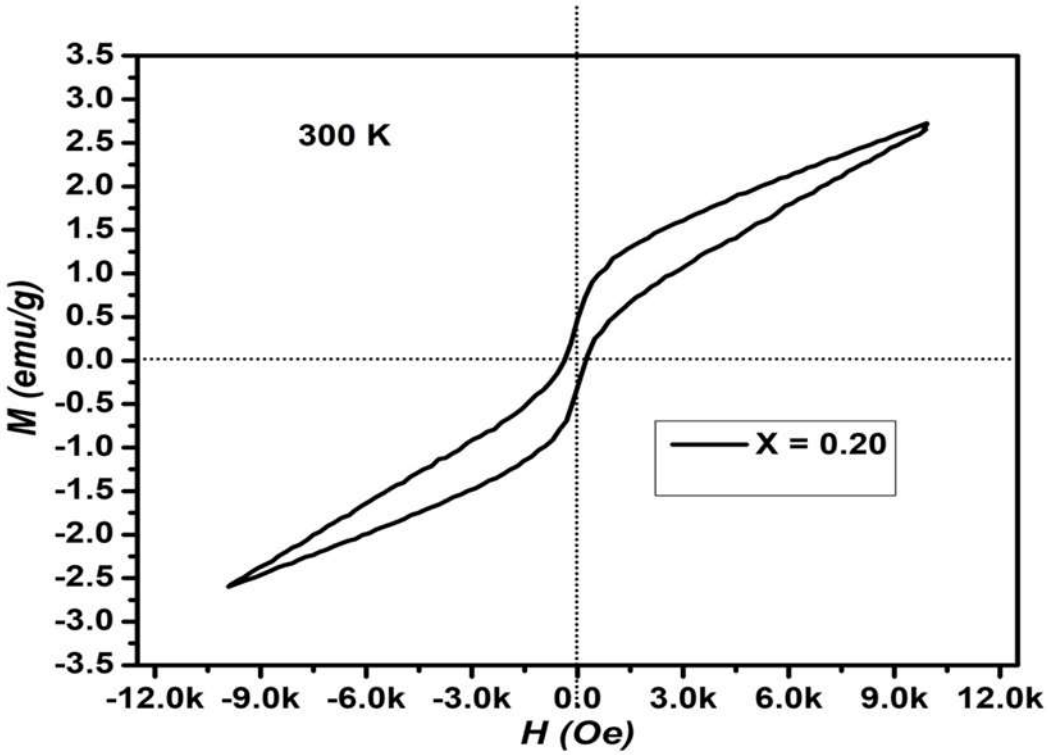

Figure 6: M-H Hysteresis loop of Gd (X = 0.20) doped $BiFeO_3$.

Figure 6displays the M-H hysteresis curves for the Gd doped BFO samples, which barely saturate near 2000 Oe and remain saturated even when the M-field is extended up to 6000 Oe. This means that the samples can withstand intense magnetic fields while keeping their magnetic properties. The higher magnetization levels in Gd-doped $BiFeO_3$ samples might be attributed to the exchange contactamid the substituted ions Gd and Fe, as well as the suppression of the canted spiral spin arrangement [19, 24].This rise in Hc and Msvalues with Gd^{3+} substitution could be attributed to a decrease in grain size and crystallite size in Gd/BFO samples, which could be an extrinsic result of the Gd doping [25]. Furthermore, the saturation magnetization (Ms) was calculated from the M-H curves at a functional magnetic field of 6000 Oe (figure 6). Overall, the results show that Gd substitution can significantly improve the magnetic properties of $BiFeO_3$ samples, and the magnetic behavior seen in these samples can be attributed to a combination of factors including crystalline size, grain size, and the exchange interaction between the dopant ion and Fe.

4. Conclusion:

Gd doped $BiFeO_3$ (X=0.20) samples prepared using the solid state reaction technique were studied for structural, dialectical and multiferroic properties. The XRD data revealed that the sample crystallized in aorthogonal for X=0.20. The double splitting of peaks at 31.83, 39.14, 51.39, and 57.04 merges into a

single peak with increasing amounts of Gd, confirming the structural transformation after substitution. The dielectric constant (ε') improves visibly as the quantity of doping increases.The variation in conductivity with frequency increases as the Gd substitution. The results of the dielectric property investigation indicate that theGdsubstitution distorted the BFO structure. The values of saturation polarization (P_s) and magnetization (M_s), respectively, have 2.256 μC/cm^2 and2.614 emu/gm, respectively. Further research on Gd doped $BiFeO_3$ is required to optimize its various electrochemical characteristics.

Acknowledgment:
The authors are also grateful to the Head, Department of Physics of BMU rohtak and CRSU Jind for providing facilities and essential support to the researchers. The authors didn't have any financial assistance for this work.

References:

[1]. S. Dunn, D. Cullen, E. Abad-Garcia, C. Bertoni, R. Carter, D. Howorth, R. W. Whatmore, Appl. Phys. Lett., **85,** 3537-3539 (2004).
[2]. J. Garra, J. M. Vohs, D. A. Bonnell, Surf. Sci.**603,** 1106-1114 (2009).
[3]. Y. H. Cho, E. K. Kim,Phys. Status Solidi (C) **6,** 782-787 (2009).
[4]. P. M. Jones, S. Dunn, J. Phys. D. **42,** 065408 (2009).
[5]. S. Dunn, D. Tiwari, Appl. Phys. Lett.**93,** 092905 (2008).
[6]. S. V. Kalinin, D. A. Bonnell, T. Alvarez, X. Lei, J.H. Ferris, S. Dunn, Q. Zhang, NanoLett.**2,**589-593 (2002).
[7]. S. V. Kalinin, Adv. Mater.**16**, 795-799 (2004).
[8]. K. Takahashi, N. Kida, M. Tonouchi, Phys. Rev. Lett. **96,** 117402 (2006).
[9]. J. Xu, G. Zhang, F. Li, X. Zhang, Q. Sun, S. Liu, F. Song, Y. Kong, X. Chen, H. Qiao, J. Yao, Z. Lijuan, Opt. Lett.**25,** 129-131 (200).
[10]. H.Wang,C.Yang,J.Lu,M.Wu,J.Su,K.Li,J.Zhang,G.Li,T.Jin,T.KamiyamaInorg.Inorg.**52,** 2388-2392 (2013).
[11]. G.Baldi,D.Bonacchi,C.Innocenti,G.Lorenzi,C.Sangregorio,J.Magn.Magn.Mater.**311,**10-16, (2007).
[12]. R.Das, K.Mandal, J.Magn. Magn.Mater.**324,** 1913-1918 (2012).
[13]. F.Kubel,H.Schmid,ActaCrystallogr.B**46,**698-702 (1990).
[14]. J.G. Park, M.D. Le, J.Jeong, S. Lee,J. Phys. Condens.Matter.**26,**433202(2014).
[15]. Y. Liu, Yuhang, First Principle Study of Multiferroic Bismuth Ferrite, (2018).
[16]. AJ. Preethi and M. Ragam, J. Adv. Dielectr. 11.06 (2021): 2130001.
[17]. I. Sosnowska, R. Przenioslo, P. Fisciier, V. A. Murashov, Acta Phys. Polonica A, **86,** 629-632 (1994).
[18]. Y. Liu, Y. Wang, J. Ma, S. Li, H. Pan, C. W. Nan, and Y. H. Lin, Progress in Materials Science 127 (2022): 100943.
[19]. S. Supriya, J. Rare Earths (2022).
[20]. R. Mansingh, R. K. Mishra, and T. Dash, AIP Conference Proceedings, 2417 (2021).

[21]. D. Bilican, E. Menendez, J. Zhang, P. Solsona, J. Fornell, E. Pellicer, J. Sort, RSCAdv.7(2017)32133.

[22]. M. Sakar , S. Balakumar ,, P. Saravanan , S.N. Jaisankar, Mater. Rese. Bull. 48(2013)2878.

[23]. F. Huang, Z. Wang, X. Lu, J. Zhang, K.Min, W.Lin, R. Ti, T. T. Xu, J. He, C.Yue,J. Zhu, Sci. Rep. **3,**1-7 (2013).

[24]. X. Xu, Y. H. Lin, P. Li, L.Shu, C. W. Nan, J. Am. Ceram. Soc. **94,** 2296-2299 (2011).

[25]. T. Gao, Z. Chen, Y. Zhu, F. Niu, Q. Huang, L. Qin, X. Sun, Y. Huang, Mater. Res. Bull. **59,** 6-12 (2014).